Journal of Power Sources 273 (2015) 810–815

Contents lists available at ScienceDirect

Journal of Power Sources

journal homepage: www.elsevier.com/locate/jpowsour

Urea-treated carbon nanofibers as efficient catalytic materials for oxygen reduction reaction

Dong Liu [a], Xueping Zhang [a, b], Tianyan You [a, *]

[a] State Key Laboratory of Electroanalytical Chemistry, Changchun Institute of Applied Chemistry, Chinese Academy of Sciences, 5625 Renmin Street, Changchun, Jilin 130022, China
[b] University of Chinese Academy of Sciences, 19A Yuquan Road, Beijing 100049, China

HIGHLIGHTS

- Nitrogen-doped carbon nanofibers (NCNFs) were prepared by post-treatment method.
- Higher content of pyrrolic-N was observed in NCNFs than that of CNFs.
- NCNFs exhibited enhanced electrocatalytic performance for oxygen reduction reaction.

GRAPHICAL ABSTRACT

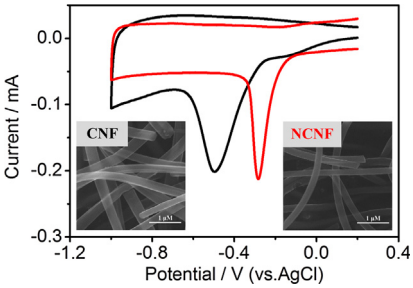

ARTICLE INFO

Article history:
Received 10 August 2014
Received in revised form
10 September 2014
Accepted 16 September 2014
Available online 28 September 2014

Keywords:
Electrospining
Nitrogen-doped carbon nanofibers
Oxygen reduction reaction
Electrocatalysis

ABSTRACT

Nitrogen-doped carbon nanofibers (NCNFs) are prepared by the thermal treatment of carbon nanofibers (CNFs) using urea as nitrogen source. Scanning electron microscopy, transmission electron microscopy and X-ray photoelectron spectroscopy have been employed to characterize the morphology and composition of CNFs and NCNFs. Compared with CNFs, NCNFs display thinner diameter, rougher surface and higher content of pyrrolic-N. As a metal-free catalyst for ORR, NCNFs exhibit comparable catalytic activity, significantly enhanced long-time stability and selectivity in comparison with commercial available Pt/C catalyst. Importantly, the self-supported NCNFs films could be conveniently utilized for electrode modification which is attractive in fuel cells. This work offers a promising metal-free catalyst as an alternative for Pt/C catalyst.

1. Introduction

High-performance catalysts for the oxygen reduction reactions (ORR) have been considered as one of critical issues in the field of fuel cells. [1,2] Pt-based catalysts have been extensively explored for the excellent electrocatalytic activity. However, high cost, poor stability and low tolerance to the crossover effect significantly limit their large-scale applications in fuel cells [3].

Recently, state-of-the-art nitrogen-doped carbon nanomaterials have attracted enormous interest as promising substitutes for Pt-based catalysts [4–6]. According to previous reports, doping nitrogen into the carbon nanomaterials could improve the interaction between carbon atoms and guest molecules, leading to the enhancement of electrocatalytic performance [7]. Up to now, the incorporation of nitrogen into the carbon matrix could be achieved during the preparation procedure or through the post-treatment of carbon nanomaterials. To dope nitrogen into the carbon structure in situ, nitrogen-doped carbon nanomaterials are always directly synthesized using nitrogen-containing precursors such as melamine [8], urea [9], pyrrole [10] and acetonitrile [11]. As for the

* Corresponding author. Tel./fax: +86 431 85262850.
E-mail address: youty@ciac.jl.cn (T. You).

http://dx.doi.org/10.1016/j.jpowsour.2014.09.104
0378-7753/

latter method, the carbons are usually treated in the ammonia (NH_3) containing atmosphere at elevated temperature. Most of these studies are focused on the nitrogen-doped carbon nanotubes and graphene; however, few investigations are aimed at the electrospun nitrogen-doped carbon nanofibers (NCNFs) [12,13]. Although carbon nanofibers (CNFs) with certain content of nitrogen could be obtained simply by the carbonization of electrospun polyacrylonitrile (PAN) nanofibers, the resulting CNFs show poor catalytic activity toward ORR. In fact, the nitrogen types in the carbons played an important role on the catalytic ability [14]. Qiu et al. carbonized the electrospun PAN nanofibers in NH_3 leading to the high content of pyrrolic-N and superior electrocatalytic activity toward ORR [15]. Our group has also synthesized electrospun NCNFs with high oxygen reduction activity by reutilizing the nitrogen-containing by-products as the nitrogen source [16]. Nevertheless, how to improve electrocatalytic activity of the electrospun CNFs for ORR is rarely studied.

Herein, we developed a simple method for the preparation of NCNFs by thermal post-treatment of electrospun carbon nanofibers using urea as nitrogen source. Compared with CNFs, the as-prepared NCNFs show smaller diameter, rougher surface and higher content of pyrrolic-N. When utilized as metal-free electrocatalyst for ORR, NCNFs exhibited comparable catalytic activity, enhanced long-time stability and better electrochemical selectivity in comparison with commercial Pt/C catalyst.

2. Experimental section

2.1. Materials

Polyacrylonitrile (PAN, M_w = 150,000) and nafion solution (5 wt.%) were purchased from Sigma–Aldrich. Potassium hydroxide (KOH), dimethylformamide (DMF, ≥99%) and methanol (≥99%) were acquired from Beijing Chemical Co.; urea and platinum on carbon (20 wt. % Pt/C, Johnson Matthey) was obtained from Aladdin Industrial Inc. and Alfa Aesar, respectively. All other reagents were used as received. All the solutions were prepared by the double-distilled water.

2.2. Preparation of self-supported NCNFs films

The pristine CNFs were prepared by the carbonization of electrospun PAN nanofibers films. Typically, electrospun PAN nanofibers were prepared by 10 wt. % PAN electrospinning solution. Stabilization and carbonization was performed as follows: (1) stabilized at 250 °C in air for 180 min, (2) heat up to 900 °C for 60 min, (3) cooled down to room temperature in nitrogen.

For NCNFs, CNFs and urea were placed in a high-temperature furnace with the mass ratio of 1: 10 as shown in Scheme 1. Then, carbonization was performed by heating up to 900 °C for 30 min with a heating-up rate of 10 °C min^{-1}, then cooling down in nitrogen atmosphere.

2.3. Characterization

Scanning electron microscopy (SEM) experiments were performed on a PHILIPS XL-30 ESEM with an accelerating voltage of 20 kV. Transmission electron microscopy (TEM) images were obtained on a TECNAI G2 with the accelerating voltage of 200 kV. X-Ray photoelectron spectroscopy (XPS) measurements were carried out on a Thermo ESCALAB 250 instrument equipped with Al Kα radiation.

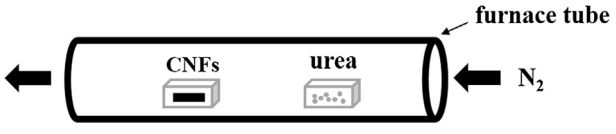

Scheme 1. The preparation of NCNFs.

2.4. Electrochemical measurements

The NCNFs film was cut to the disk shape, and then adhered onto the glassy carbon electrode (GCE) using 0.5 wt. % nafion solution. For comparison, commercial Pt/C catalyst and pristine CNFs suspension was prepared in ethanol with the content of 4 mg mL^{-1}. The suspension was casted on the GCE, and nafion solution was also used. All the electrochemical measurements were performed on a CHI 832C electrochemical workstation, using a three-electrode system comprising by the modified GCE as the working electrode, a Pt plate as the counter electrode, and an Ag/AgCl (saturated KCl) electrode as reference electrode. The sample-modified working electrode was prepared by the same method as for CVs. The electrolyte saturated with O_2 or N_2 was bubbled for at least 30 min before experiments.

3. Results and discussion

Scanning electron microscopy (SEM) and transmission electron microscopy (TEM) were employed to characterize the structure and morphology of CNFs and NCNFs. The average diameter of NCNFs (ca. 232 nm) displays an obviously decrease in contrast to that of CNFs (ca. 303 nm) (Fig. 1). Additionally, a rougher surface for NCNFs could be observed in comparison with CNFs (Fig. 1C and D). These results may origin from the surface etching and nitrogen doping by nitrogen-containing gaseous compounds, particularly NH_3, formed during the decomposition process of urea [17]. The radicals (such as NH and NH_2) generated by NH_3 at elevated temperature could replace the oxygen-containing groups by nitrogen-containing groups on the surface of carbons [18,19].

The XPS spectra for CNFs (Fig. 2A) and NCNFs (Fig. 2C) demonstrate the presence of C 1s (284 eV), O 1s (540 eV) and N 1s (400 eV). The nitrogen content of CNFs and NCNFs were estimated to be 5.5% and 2.1%, respectively. Moreover, it is reported that the forms of nitrogen in carbons play a more important role compared with the content of nitrogen for catalytic properties [15]. To exploit the forms of nitrogen in CNFs and NCNFs, high-resolution N 1s spectra measurements were carried out. Generally, the nitrogen doped into carbon nanomaterials could be in the forms of pyridinic-N (398.7 ± 0.3 eV), pyrrolic-N (400.4 ± 0.3 eV) and graphitic-N (401.4 ± 0.3 eV) [20,21]. All these forms of nitrogen were found in CNFs and NCNFs (Fig. 2B and D). It is noteworthy that higher content of pyrrolic-N was observed in NCNFs (53%) than that in CNFs (26%) which is in good agreement with our previous work [16].

Benefiting from the unique self-supported structure, NCNFs films could be directly utilized as the electrode for electrochemical experiments. In this work, the electrocatalytic performance of NCNFs was evaluated by ORR using a NCNFs modified GCE as working electrode in the O_2-saturated 0.1 M KOH solution (Fig. 3). The ORR peak potential at NCNFs is −0.27 V, significantly positive than that at CNFs (−0.50 V), suggesting a superior oxygen reduction ability. Moreover, rotating disk electrode (RDE) measurements were also performed to study the electrocatalytic activity at NCNFs, commercial Pt/C and CNFs toward ORR. As shown in Fig. 3B, the onset potential at CNFs, NCNFs and Pt/C is −0.17 V, −0.031 V and 0.048 V, respectively. Accordingly, the ORR onset potential at NCNFs is only ca. 79 mV negatively than that at Pt/C, indicating a comparable catalytic activity toward ORR.

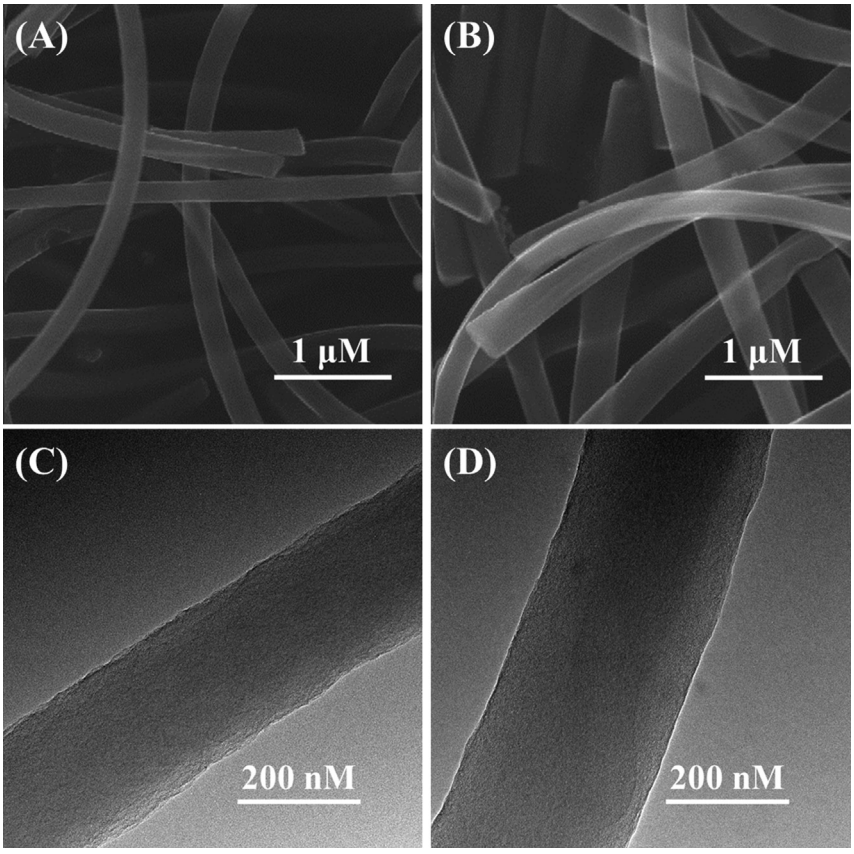

Fig. 1. SEM images of NCNFs (A) and CNFs (B); TEM images of NCNFs (C) and CNFs (D).

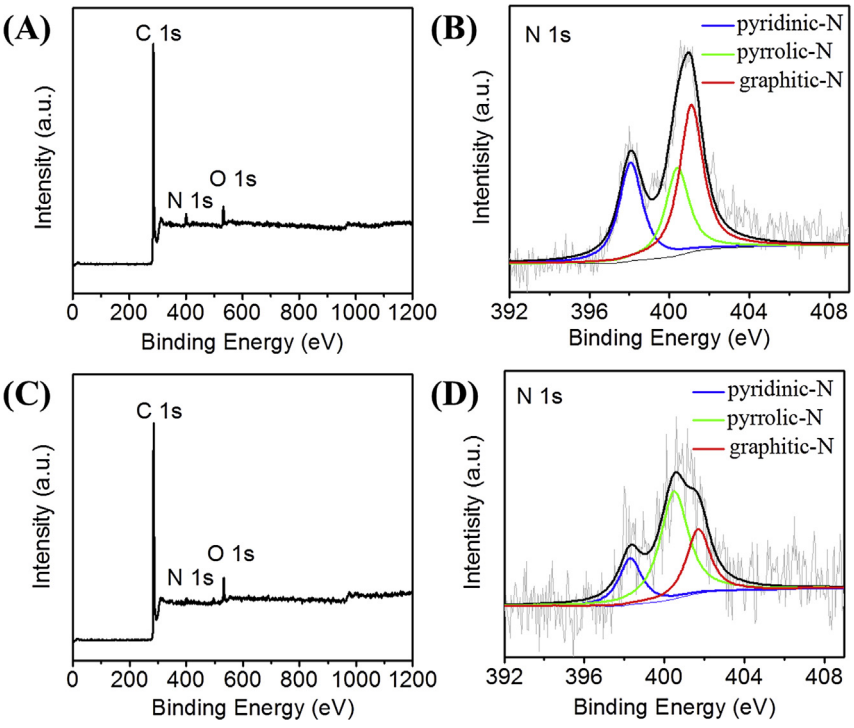

Fig. 2. X-ray photoelectron spectra and corresponding high-resolution N 1s spectra for CNFs (A, B) and NCNFs (C, D).

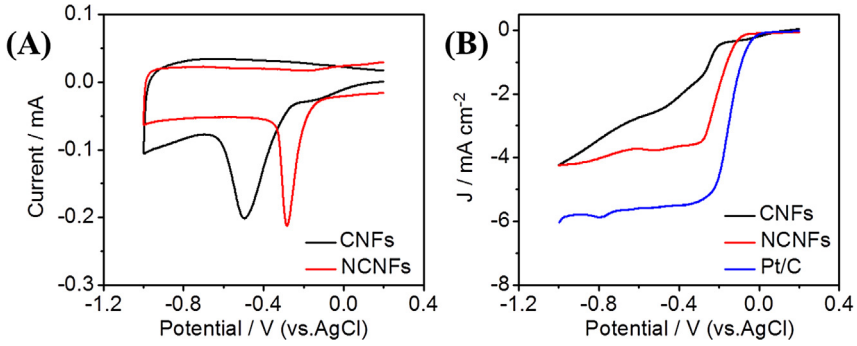

Fig. 3. (A) Cyclic voltammograms of CNFs and NCNFs in O_2-saturated 0.1 M solution of KOH at a scan rate of 50 mV s^{-1}. (B) Rotating disk electrode voltammograms of CNFs, NCNFs and Pt/C in O_2-saturated 0.1 M solution of KOH at a scan rate of 10 mV s^{-1} at 1600 rpm.

ORR in basic solution includes the $2e^-$ reduction pathway with HO_2^- as intermediate specie, and $4e^-$ reduction pathway to directly produce OH^- [22,23].

$$4e^- \text{pathway} \quad O_2 + 2H_2O + 4e^- \rightarrow 4OH^- \tag{1}$$

$$2e^- \text{pathway} \quad O_2 + H_2O + 2e^- \rightarrow HO_2^- + OH^- \tag{2}$$

$$HO_2^- + H_2O + 2e^- \rightarrow 3OH^- \tag{3}$$

To investigate the ORR electrochemical process at NCNFs, reaction kinetics was studied by RDE measurements. The electron transfers number (n) in the ORR process at NCNFs and CNFs are obtained using Koutecky–Levich equations which describes a linear relationship between the current density (J), kinetic current density (J_k), and the rotation speed (ω) (Equations (4)–(5)) [24].

$$\frac{1}{J} = \frac{1}{J_K} + \frac{1}{J_L} = \frac{1}{J_K} + \frac{1}{\beta\omega^{0.5}} \tag{4}$$

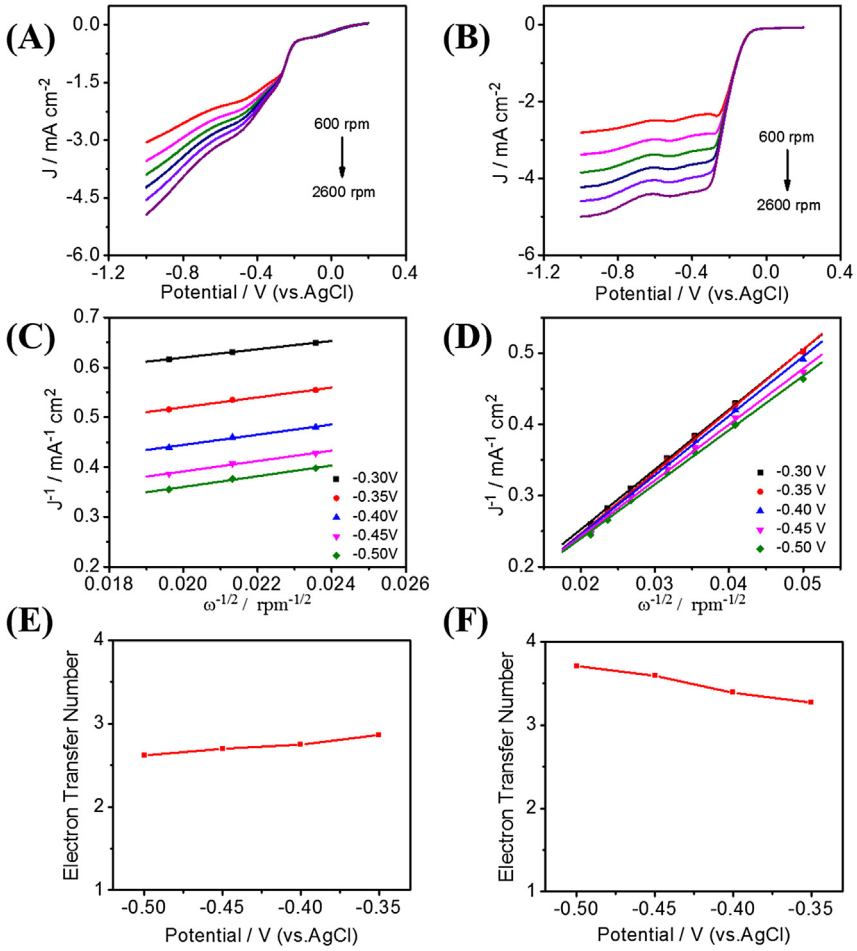

Fig. 4. Rotating disk electrode voltammograms recorded for CNFs (A) and NCNFs (B) in O_2-saturated 0.1 M solution of KOH at different rotation rates with a sweep rate of 10 mV s^{-1}; Koutecky–Levich plot of J^{-1} versus $\omega^{-1/2}$ at different electrode potentials for CNFs (C) and NCNFs (D); the dependence of the electron transfer number on the potential for both the CNFs (E) and NCNFs (F).

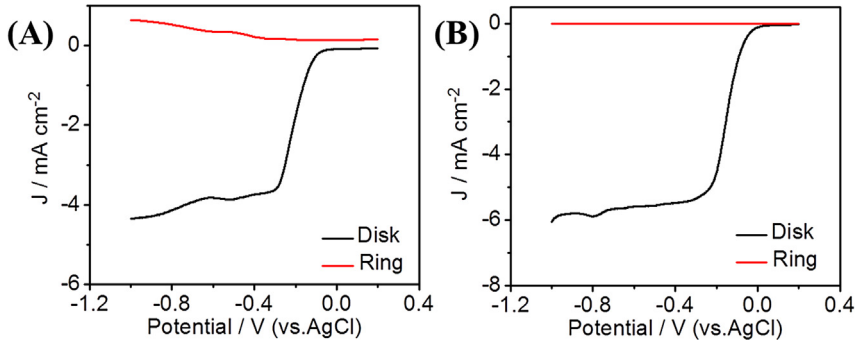

Fig. 5. Rotating disk-ring electrode test at NCNFs and Pt/C in O_2-saturated 0.1 M solution of KOH. Scan rate: 10 mV s^{-1}. Rotation rate: 1600 rpm.

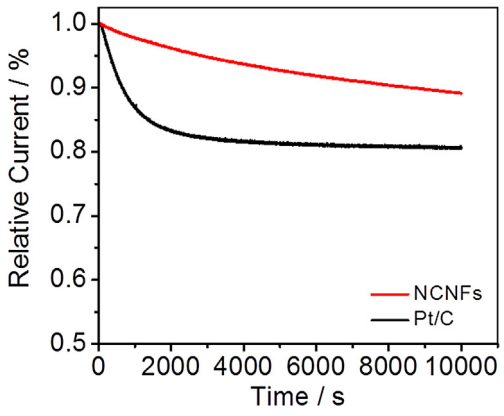

Fig. 6. Chronoamperometric response of NCNFs and Pt/C at −0.26 V in O_2-saturated 0.1 M KOH with a rotation rate of 1600 rpm.

$$\beta = 0.2nF(D_0)^{\frac{2}{3}}C_0\nu^{\left(-\frac{1}{6}\right)} \quad (5)$$

D_0 is the diffusion coefficient of O_2 in 0.1 M KOH (1.73×10^{-5} cm^2 s^{-1}); F, ν and C_0 is the Faradic constant (96,486 C mol^{-1}), kinematic viscosity (0.01 cm^2 s^{-1}) and concentration of O_2 (1.21×10^{-6} mol L^{-1}), respectively.

The linear sweep voltammetric curves of NCNFs and CNFs with rotation speeds ranging from 600 to 2600 rpm are shown in Fig. 4. According to Equations (4) and (5), the values of n for NCNFs and CNFs at different potentials could be obtained which shows the ORR at NCNFs processed a close $4e^-$ pathway (Fig. 4E–F). For instance, the n value is 3.7 at −0.5 V for NCNFs while 2.6 for CNFs.

Rotating disk-ring electrode (RRDE) measurements were further applied to investigate the HO_2^- production percentage ($y_{peroxide}$). The value of $y_{peroxide}$ and n was calculated to be 37% and 3.2 for NCNFs at −0.5 V (Fig. 5) [25]. Obviously, the value of n is consistent with that obtained by Koutecky–Levich equations, demonstrating a close $4e^-$ pathway at NCNFs.

NCNFs could catalyse ORR with a higher long-time durability than Pt/C catalyst according to the stability test. After a continuous operation of 10,000 s, 89% of the current density remained at NCNFs, while 81% remained at commercial Pt/C (Fig. 6). In addition, we have performed the accelerated degradation testing with cyclic voltammograms ranging from −1.0 V to 0.3 V at 100 mV s^{-1} in O_2-saturated 0.1 M KOH for over 5100 cycles. The results demonstrate that the $E_{1/2}$ only negatively shifted ca. 32 mV after 5100th potential cycling, confirming the superior long-time stability.

The catalytic selectivity is another important issue which should be considered for ORR catalysts. In our work, the crossover effect of methanol was investigated at NCNFs and commercial Pt/C catalyst. As shown in Fig. 7A, no noticeable changes are observed on the electrocatalytic activity of NCNFs. In contrast, a strong response to methanol at Pt/C could be observed while the cathodic peak of ORR vanished (Fig. 7B). Thus, the as-prepared NCNFs show better electrocatalytic selectivity for ORR than Pt/C catalyst which could be attributed to the lower potential for ORR at NCNFs compared with that for oxidation of the methanol [26].

As described above, the as-obtained NCNFs display higher electrocatalytic activity than that of CNFs toward ORR. Despite the decreased content of nitrogen in NCNFs compared with CNFs, previous reports have deduced that the formations of surface nitrogen groups in N-doped carbon nanomaterials are of great importance on the electrochemical properties of carbons. Benefiting from the long pair electron, pyrrolic-N at the edges of graphene layers could significantly enhance the charge mobility and donor–acceptor properties of the carbon nanomaterials [27]. Thus, an improvement of catalytic activity could be expected benefited from the high content of pyrrolic-N [16,28]. In this work,

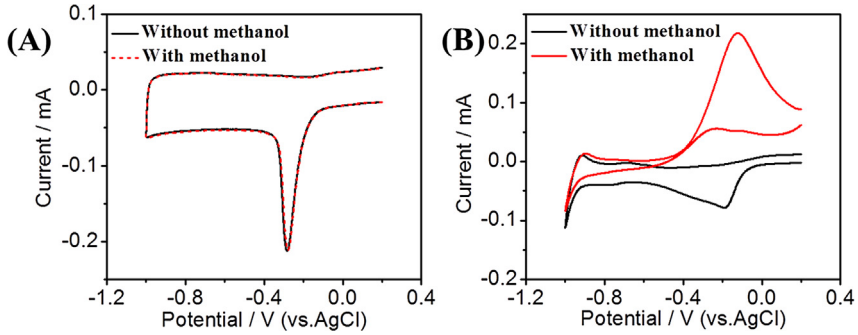

Fig. 7. Cyclic voltammograms of (A) NCNFs and (B) Pt/C in N_2- and O_2-saturated 0.1 M solution of KOH, in O_2-saturated 0.1 M solution of KOH upon the addition of CH_3OH (3 M) at a scan rate of 50 mV s^{-1}.

we attributed the enhanced oxygen reduction ability of NCNFs to the high content of pyrrolic-N.

4. Conclusion

Novel self-supported nitrogen-doped carbon nanofibers are successfully prepared via a simple thermal post-treatment of electrospun carbon nanofibers. In this study, urea, as a facile and economical nitrogen source, is used for the nitrogen doping and surface etching. The morphology and composition characterization reveal that the nitrogen-doped carbon nanofibers show thin diameter, rough surface and high content of pyrrolic-N. Used as the catalyst for oxygen reduction reaction, the nitrogen-doped carbon nanofibers exhibit comparable electrocatalytic activity, much better stability and selectivity in comparison with commercial Pt/C catalyst. The nitrogen-doped carbon nanofibers with unique self-supported structure and high electrochemical property could be a potential substitute for Pt/C catalyst in fuel cell.

Acknowledgements

We are grateful for the financial support from the National Natural Science Foundation of China (No. 21222505).

References

[1] B.C.H. Steele, A. Heinzel, Nature 414 (2001) 345–352.
[2] D.W. Wang, D.S. Su, Energy Environ. Sci. 7 (2014) 576–591.
[3] J.L. Shui, C. Chen, J.C.M. Li, Adv. Funct. Mater. 21 (2011) 3357–3362.
[4] K.P. Gong, F. Du, Z.H. Xia, M. Durstock, L.M. Dai, Science 323 (2009) 760–764.
[5] T. Kamata, D. Kato, S. Hirono, O. Niwa, Anal. Chem. 5 (2013) 9845–9851.
[6] M.K. Liu, Y.F. Song, S.X. He, W.W. Tjiu, J.S. Pan, Y.Y. Xia, T.X. Liu, ACS Appl. Mater. Interfaces 6 (2014) 4214–4222.
[7] P.H. Matter, L. Zhang, U.S. Ozkan, J. Catal. 239 (2006) 83–96.
[8] Z.J. Wang, R.R. Jia, J.F. Zheng, J.H. Zhao, L. Li, J.L. Song, Z.P. Zhu, ACS Nano 5 (2011) 1677–1684.
[9] C. Xiong, Z.D. Wei, B.S. Hu, S.G. Chen, L. Li, L. Guo, W. Ding, X. Liu, W.J. Ji, X.P. Wang, J. Power Sources 215 (2012) 216–220.
[10] L.F. Chen, X.D. Zhang, H.W. Liang, M.G. Kong, ACS Nano 6 (2012) 7092–7102.
[11] T.X. Cui, R.T. Lv, Z.H. Huang, H.W. Zhu, F.Y. Kang, K.L. Wang, D.H. Wu, Carbon 50 (2012) 3659–3665.
[12] Z.H. Sheng, X.Q. Zheng, J.Y. Xu, W.J. Bao, F.B. Wang, X.H. Xia, Biosens. Bioelectron. 34 (2012) 125–131.
[13] W. Fan, Y.Y. Xia, W.W. Tjiuc, P.K. Pallathadka, C.B. He, T.X. Liu, J. Power Sources 243 (2013) 973–981.
[14] S.M. Unni, S. Devulapally, N. Karjulea, S. Kurungot, J. Mater. Chem. 22 (2010) 23506–23513.
[15] Y.J. Qiu, J. Yu, T.N. Shi, X.S. Zhou, X.D. Bai, J.Y. Huang, J. Power Sources 196 (2011) 9862–9867.
[16] D. Liu, X.P. Zhang, Z.C. Sun, T.Y. You, Nanoscale 5 (2013) 9528–9531.
[17] X.Q. Wang, J.S. Lee, Q. Zhu, J. Liu, Y. Wang, S. Dai, Chem. Mater. 22 (2010) 2178–2180.
[18] B. Stohr, H.P. Boehm, R. Schlogl, Carbon 29 (1991) 707–720.
[19] C.L. Mangun, K.R. Benak, J. Economy, K.L. Foster, Carbon 39 (2001) 1809–1820.
[20] J.R. Pels, F. Kapteijn, J.A. Moulijn, Q. Zhu, Carbon 33 (1995) 1641–1653.
[21] C. Ronning, H. Feldermann, R. Merk, H. Hofsäss, Phys. Res. B 58 (1998) 2207–2215.
[22] X. Xu, S.J. Jiang, Z. Hu, S.Q. Liu, ACS Nano 4 (2010) 4292–4298.
[23] L. Yu, X.L. Pan, X.M. Cao, P. Hu, X.H. Bao, J. Catal. 282 (2011) 183–190.
[24] D.S. Yu, Q. Zhang, L.M. Dai, J. Am. Chem. Soc. 132 (2010) 15127–15129.
[25] D.S. Geng, Y. Chen, Y.G. Chen, Y.L. Li, R.Y. Li, X.L. Sun, S.Y. Ye, S. Knights, Energy Environ. Sci. 4 (2011) 760–764.
[26] H.F. Cui, J.S. Ye, X. Liu, W.D. Zhang, F.S. Sheu, Nanotechnology 17 (2006) 2334–2339.
[27] S. Maldonado, S. Morin, K.J. Stevenson, Carbon 44 (2006) 1429–1437.
[28] L. Zhang, Z. Xia, J. Phys. Chem. C 115 (2011) 11170–11176.